Hindawi Publishing Corporation
Journal of Nanomaterials
Volume 2016, Article ID 9451319, 5 pages
http://dx.doi.org/10.1155/2016/9451319

Research Article

Electrical Properties of Polytypic Mg Doped GaAs Nanowires

N. Cifuentes,[1] E. R. Viana,[2] H. Limborço,[1] D. B. Roa,[1,3] A. Abelenda,[1,4] M. I. N. da Silva,[1] M. V. B. Moreira,[1] G. M. Ribeiro,[1] A. G. de Oliveira,[1] and J. C. González[1]

[1]*Departamento de Física, Instituto de Ciências Exatas, Universidade Federal de Minas Gerais, Avenida Presidente Antônio Carlos 6627, Pampulha, 31270-901 Belo Horizonte, MG, Brazil*
[2]*Departamento Acadêmico de Física, Universidade Tecnológica Federal do Paraná, Campus Curitiba, Avenida Sete de Setembro 3165, Rebouças, 80230-901 Curitiba, PR, Brazil*
[3]*Departamento de Física, Instituto Federal de Minas Gerais, Campus Ouro Preto, Rua Pandiá Calógeras 898, Bauxita, 35400-000 Ouro Preto, MG, Brazil*
[4]*Facultad de Física-ICTM, Universidad de La Habana, Colina Universitária, 10400 La Habana, Cuba*

Correspondence should be addressed to J. C. González; gonzalez@fisica.ufmg.br

Received 10 April 2016; Revised 20 June 2016; Accepted 11 July 2016

Academic Editor: Yu-Lun Chueh

The electrical transport properties of individual Mg doped GaAs nanowires are investigated. It is shown that Mg can be successfully used as a nontoxic p-type dopant in GaAs nanowires. The doping levels, expanding over two orders of magnitude, and free holes mobility in the NW were obtained by the analysis of field effect transistors transfer curves. The temperature dependence of the electrical resistivity above room temperature shows that the polytypic structure of the NWs strongly modifies the NWs charge transport parameters, like the resistivity activation energy and holes mobility. At lower temperatures the NWs exhibit variable range hopping conduction. Both Mott and Efros-Shklovskii variable range hopping mechanisms were clearly identified in the nanowires.

1. Introduction

Semiconductor nanowires (NWs) of III-V compounds [1–5] are promising nanostructures for optoelectronic devices applications [5, 6]. However, the influence of temperature as well as the polytypism in the transport mechanisms of p-type doped III-V NWs has been barely investigated [6–15]. In this work, we present a study of the electrical transport properties of polytypic and p-type Mg doped GaAs NWs near and above room temperature.

Beryllium is the standard p-type dopant in III-V compounds thin films due to its near-unity sticking coefficient and low vapor pressure [16, 17]. However, due to its high toxicity, it is important to find nontoxic and noncarcinogenic alternatives. Mg is a known nontoxic shallow acceptor for III-V compounds [13, 16, 17], but the low incorporation coefficient at the usual growth temperatures had limited its use as a viable p-type dopant in III-V thin films [17]. However, III-V NWs are usually grown at lower temperatures [6, 8] allowing higher doping levels to be reached in those nanostructures. The use of Mg as p-type dopant presents the additional advantage of simplifying the integration of diverse III-V since it dopes all III-V compounds, including nitrides semiconductors. We have recently demonstrated the feasibility of growing Mg doped GaAs NWs [18] and studied their optical properties [19, 20]. In our studies the optical emission was dominated by Zincblende/Wurtzite (ZB/WZ) polytypism along the NWs that creates type-II optical transitions between electrons localized at the bottom of the conduction band of ZB segments and holes localized at the top of the valence band in adjacent WZ segments [18–20]. Luminescence related to the Mg acceptors was observed on GaAs thin films, but not in the NWs. To further understand the polytypism effects on the electronic process in p-type doped GaAs NWs a deeper study of the electrical transport in individual NWs is carried out here as a function of temperature.

2. Experimental Details

GaAs NWs and thin films were grown on GaAs (111)B substrates in a solid source *Riber 2300 R&D* MBE reactor.

NWs were grown on drop-coated substrates with a water suspension of 5 nm thick colloidal Au nanoparticles, while the thin films were grown on uncoated substrates. The substrates were In glued to a Mo sample holder and outgassed at 350°C by two hours in UHV (1.2×10^{-10} Torr). Afterwards, the sample holder was transferred to the growth chamber where the protective oxide of the substrates was removed by heating at 625°C, during 20 minutes, and under an As_4 beam equivalent pressure (BEP) of 3.4×10^{-5} Torr. The NWs growth was performed during 90 min, with an As_4 BEP of 3.4×10^{-5} Torr, a Ga BEP of 7.2×10^{-7} Torr, and at a nominal growth rate for thin films of 1 μm/h. NWs and thin films were p-type doped by using a Mg effusion cell.

The morphology and crystalline structure of the nanowires was investigated by transmission electron microscopy (TEM) by using a *Tecnai G2-20 SuperTwin FEI* high resolution electron microscope.

For transport measurements, individual NWs back-gate FETs were built by mechanically transferring the NWs onto a heavily doped Si substrate covered by a 300 nm thick SiO_2 layer. Standard photolithography methods were used to define contact lines with a lateral separation of 3 to 4 μm, connecting individual NWs to macroscopic contact pads of $600 \times 600\ \mu m^2$. The NWs were etched in HCl/H_2O 1 : 10 solution for 20 s, followed by a 60 s surface passivation in a heated (40°C) NH_4Se/H_2O 1 : 10 solution. Electrical contacts to the NWs were made by evaporating a Cr (10 nm)/Au (200 nm) bilayer after etching and passivation. The devices were placed in an *Oxford CF1200 liquid He-7 cryostat*, with a precise *Oxford ITC503* temperature-controller. *Keithley 237 source-meter* and *Keithley 230 voltage-source* were used in the electrical measurements using homemade software.

3. Results and Discussion

Figure 1(a) shows a transmission electron microscopy (TEM) image of an approximately 40 nm thick GaAs NW. Alternating ZB/WZ (clear and dark) regions [20] along the NW axis are already visible in this magnification, as well as the catalyst gold particle at the top of the NW. The observed NWs presented ZB and WZ regions oriented at the ⟨011⟩ and ⟨1$\bar{2}$10⟩, respectively. A selected area electron diffraction (SAED) pattern from the central region of the NW is shown in Figure 1(b). This diffraction pattern is actually a composition of three different patterns with zone axes: ZB [0$\bar{1}$1], WZ [1$\bar{2}$10], and ZB [01$\bar{1}$]. Therefore, not only alternated ZB/WZ regions exist in the GaAs NWs, but there is also ZB segments rotated with respect to each other. A HRTEM image of a portion of the GaAs NW is shown in Figure 1(c). It is possible to determine the structure and orientation of any segment along the NW by correlating the SAED patterns and the Fast Fourier Transform (FFT) of the region of interest in the HRTEM image.

The concentration and mobility of free holes in the FET channel of four individual NWs (NW1 to NW4) were determined by using the standard analysis of the FET transfer characteristic [21–24]. Figure 2 shows a graph of the holes mobility as a function of holes concentration for different NWs and

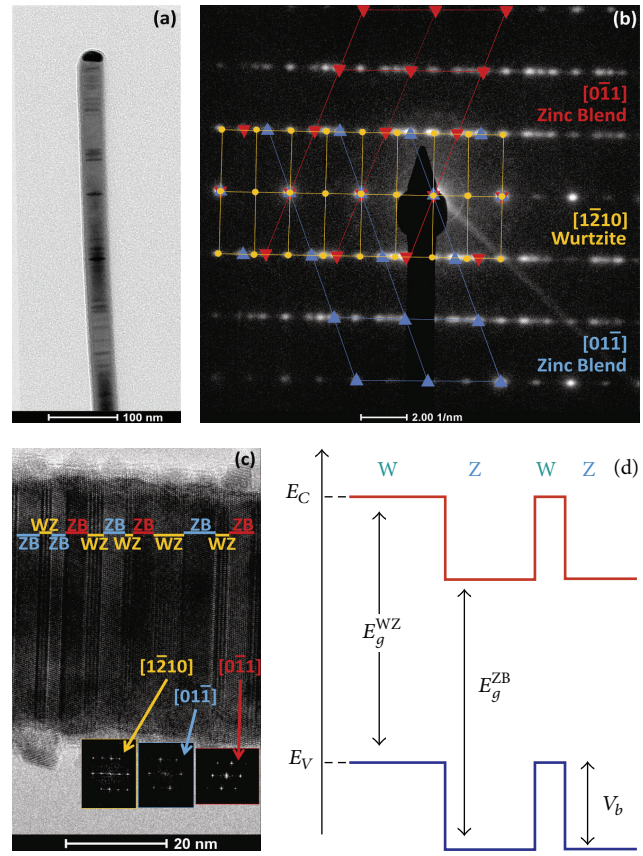

Figure 1: (a) TEM image of a Mg doped GaAs NW. (b) SAED pattern of the NW, showing a superposition of three different oriented crystalline segments: GaAs ZB [0$\bar{1}$1], GaAs WZ [1$\bar{2}$10], and GaAs ZB [01$\bar{1}$]. The growth direction is ⟨111⟩ and ⟨0001⟩ for the ZB and WZ regions, respectively. (c) HRTEM of the NW and FFT (insets) of three regions that can be correlated to the SAED pattern in (b). (d) Band alignment diagram of the NW.

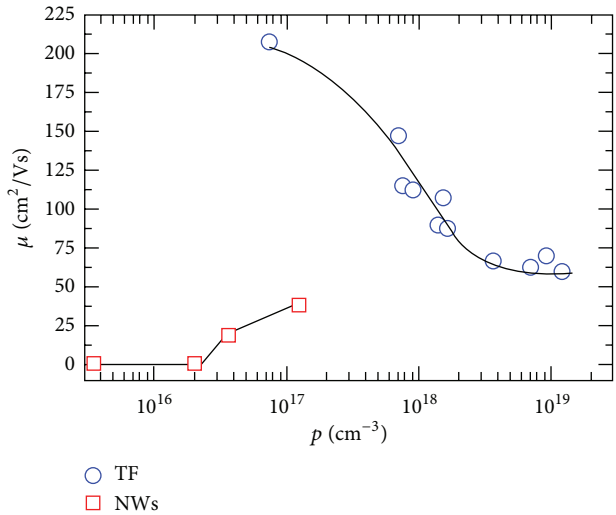

Figure 2: Hole mobility as a function of hole concentration for several Mg doped GaAs nanowires (NWs) and thin films (TF).

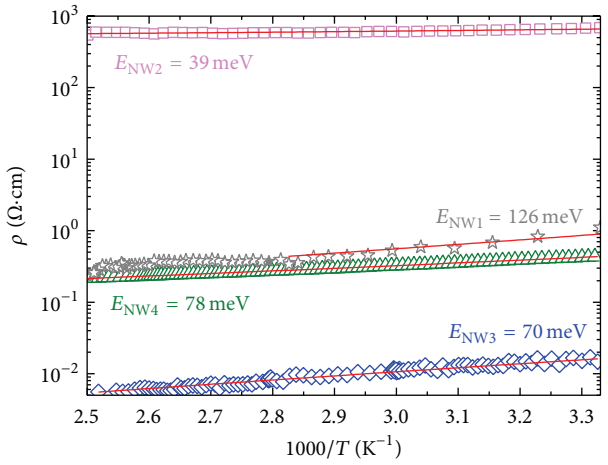

FIGURE 3: Temperature dependence of the electrical resistivity $\rho(T)$ of several individual Mg doped GaAs NWs. The red lines correspond to the fitting of the experimental data using (1).

thin film samples. The values of μ obtained for the thin films decrease with the holes concentration due to defect scattering [9, 25]. However, the opposite trend is observed for the NWs. These contradictions reveal that the scattering mechanism of free holes in the NWs is significantly different from bulk GaAs. The solid lines in Figure 2 are only guides to the eyes.

Figure 3 shows the Arrhenius plot of the electrical resistivity $\rho(T)$ of individual NWs (NW1 to NW4) between 400 and 300 K. The electronic transport in this temperature region in bulk p-type GaAs is due to free holes in the valence band, thermally ionized from shallow acceptors levels. In our case, these acceptors levels are created by Mg impurities and present ionization energy of 28 meV [15–17].

In bulk GaAs the holes mobility above 200 K is dominated by lattice scattering: $\mu_{\text{lat}}(T) = \mu_0(297\,\text{K}/T)^{\alpha}$, where μ_0 and $\alpha = 2.3$ are constants [26, 27], as well as by ionized impurity scattering μ_{ii} [28]. The Matthiessen rule $[\mu(T)]^{-1} = [\mu_{\text{lat}}(T)]^{-1} + [\mu_{\text{ii}}]^{-1}$ can be applied in order to found the total holes mobility $\mu(T)$ [26–28]. Therefore the electrical resistivity can be approximately expressed by [29]

$$\rho(T) = \rho_0 \left[\mu(T)\right]^{-1} T^{-3/2} \exp\left(\frac{E_i}{k_B T}\right), \quad (1)$$

where ρ_0 is a constant, k_B is the Boltzmann constant, and E_i is the ionization energy of the Mg acceptors.

The values of E_i (presented in Figure 3 and Table 1) obtained from the fitting using (1) are significantly different from the expected 28 meV value of the ionization energy of Mg acceptors. This new disagreement also indicates that the transport mechanism of free holes in the NWs is significantly different from the transport in bulk GaAs.

Both discrepancies, in resistivity activation energy and in mobility values, can be explained in terms of the type-II band alignment in the NWs caused by the WZ/ZB polytypism [18–20]. A simplified band alignment diagram of a section of a GaAs NW is shown in Figure 1(d). Due to this band alignment, WZ segments act as electron potential wells, while

TABLE 1: Values of the ionization energy E_i, the hopping parameters T_M and T_{ES}, and the corresponding holes mobility μ and concentration p.

NW	E_i (meV)	T_M (K)	T_{ES} (K)	μ (cm^2/Vs)	p (cm^{-3})
1	126	2×10^6	27	0.34	3.5×10^{15}
2	39	5×10^5	35	0.26	2.1×10^{16}
3	70	2×10^7	484	18.4	3.8×10^{16}
4	78	1×10^4	24	37.3	1.3×10^{17}

ZB segments act as hole potential wells. The WZ segments will behave as barriers to overcome by the holes in order to be transported along the NWs by a low electric field. Therefore, the transport of free holes in the NW is a complex process influenced not only by the ionization energy of Mg acceptors, but also by the scattering mechanism in the WZ segments and to overcome the WZ barriers.

As the temperature drops most of the free holes are recaptured by acceptors, conduction at the valence band becomes less important, and holes' hopping between acceptors states turns into the main conduction mechanism [30, 31]. In our case, the NWs are thick enough to sustain 3D hopping [30] likewise bulk GaAs.

At temperatures below 280 K, conduction by Mott variable range hopping (Mott-VRH) [31] can be identified in the NWs. The resistivity in this regime is given by

$$\rho_M(T) = \rho_{0M} T^{1/2} \exp\left(\frac{T_M}{T}\right)^{1/4}$$
$$T_M = \left(\frac{\beta_M}{\xi^3 N(E_F)}\right), \quad (2)$$

where T_M measures the degree of disorder in the material, ρ_{0M} and $\beta_M = 18.1$ are constants [32], ξ is the localization length which characterizes the hopping probability between sites, and $N(E_F)$ is the density of states near de Fermi level.

The Arrhenius plots of $\rho \cdot T^{-1/2}$ versus $T^{-1/4}$, between 280 and 55 K, is shown in Figure 4. A linear region, with characteristic temperature $T_M = 3 \times 10^4$ K, can be observed showing that Mott-VRH is the dominant conduction mechanism.

As temperature further decreases, the Coulomb effect becomes more important and the conductivity crosses over from Mott-VRH to Efros-Shklovskii VRH (ES-VRH) regime where the resistivity is given by [32]

$$\rho_{\text{ES}}(T) = \rho_{0\text{ES}} T \exp\left(\frac{T_{\text{ES}}}{T}\right)^{1/2}$$
$$T_{\text{ES}} = \left(\frac{\beta_{\text{ES}} e^2}{\varepsilon k_B \xi}\right), \quad (3)$$

where ε is the dielectric constant and $\rho_{0\text{ES}}$ and $\beta_{\text{ES}} = 2.8$ are constants [32].

The Arrhenius plots of $\rho \cdot T^{-1}$ versus $T^{-1/2}$ for temperatures below 11 K is shown in Figure 4. A linear region, with $T_{\text{ES}} = 27$ K, can be observed below 11 K. However,

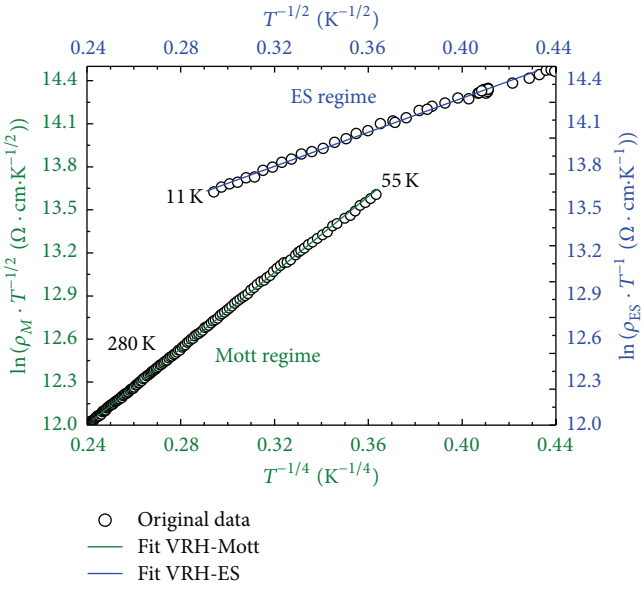

FIGURE 4: Temperature dependence of the hopping conduction in a Mg doped GaAs NW. The green line corresponds to the fitting of $\rho \cdot T^{-1/2}$ versus $T^{-1/4}$ plot in the Mott-VRH region using (2). The blue line corresponds to the fitting of $\rho \cdot T^{-1}$ versus $T^{-1/2}$ in the ES-VRH region using (3).

measurements at much lower temperatures are necessary to precisely evaluate the ES-VRH transport regime.

The above-presented analysis was applied to four NWs with different doping levels (see Table 1). Large values of T_M indicate a large degree of disorder in the NWs. The variations of the hopping transport parameters from wire to wire are an additional indication of the effect of polytypism in the charge transport in the NWs.

4. Conclusions

In conclusion, it was shown that Mg can be used as a nontoxic p-type dopant in GaAs NWs. It was also found that the mobility of free holes, as well as the resistivity activation energy above room temperature, is strongly influenced by the polytypism in the NWs. Two variable range hopping conduction mechanisms were observed at low temperatures, starting from Mott-VRH and transiting to ES-VRH as temperature drops. Further studies are necessary in order to fully understand the effects of the polytypism in the electrical transport mechanism in NWs.

Competing Interests

The authors declare that they have no competing interests.

Acknowledgments

The authors would like to acknowledge the Center of Microscopy at the Universidade Federal de Minas Gerais for providing the equipment and technical support for experiments involving electron microscopy. The financial support of the Brazilian funding agencies CAPES (Grants 1566/2010 and 88881.068066/2014-01), CNPq (Grants 302437/2014-2 and 474010/2013-9), and FAPEMIG (Grant APQ-01692-13) is also acknowledged.

References

[1] J. C. González, M. I. N. Da Silva, X. S. Lozano et al., "Structural and optical characterization of strained free-standing InP nanowires," *Journal of Nanoscience and Nanotechnology*, vol. 6, no. 7, pp. 2182–2186, 2006.

[2] V. Lopez-Richard, J. C. González, F. M. Matinaga et al., "Markovian and non-markovian light-emission channels in strained quantum wires," *Nano Letters*, vol. 9, no. 9, pp. 3129–3136, 2009.

[3] J. C. González, A. Malachias, R.-R. Andrade, J. C. De Sousa, M. V. B. Moreira, and A. G. De Oliveira, "Direct evidences of enhanced Ga interdiffusion in InAs vertically aligned free-standing nanowires," *Journal of Nanoscience and Nanotechnology*, vol. 9, no. 8, pp. 4673–4678, 2009.

[4] R.-R. Andrade, A. Malachias, G. Kellerman et al., "Experimental evidence and modified growth model of alloying in In x Ga1-xAs nanowires," *Journal of Physical Chemistry C*, vol. 116, no. 46, pp. 24777–24783, 2012.

[5] J. C. Shin, P. K. Mohseni, K. J. Yu et al., "Heterogeneous integration of InGaAs nanowires on the rear surface of Si solar cells for efficiency enhancement," *ACS Nano*, vol. 6, no. 12, pp. 11074–11079, 2012.

[6] G. E. Cirlin, A. D. Bouravleuv, I. P. Soshnikov et al., "Photovoltaic properties of p-Doped GaAs nanowire arrays grown on n-Type GaAs(111)B substrate," *Nanoscale Research Letters*, vol. 5, no. 2, article 360, 2010.

[7] N. Han, F. Wang, J. J. Hou et al., "Controllable p–n switching behaviors of GaAs nanowires via an interface effect," *ACS Nano*, vol. 6, no. 5, pp. 4428–4433, 2012.

[8] C. Gutsche, I. Regolin, K. Blekker, A. Lysov, W. Prost, and F. J. Tegude, "Controllable p-type doping of GaAs nanowires during vapor-liquid-solid growth," *Journal of Applied Physics*, vol. 105, no. 2, Article ID 024305, 2009.

[9] M. Piccin, G. Bais, V. Grillo et al., "Growth by molecular beam epitaxy and electrical characterization of GaAs nanowires," *Physica E: Low-Dimensional Systems and Nanostructures*, vol. 37, no. 1-2, pp. 134–137, 2007.

[10] J. Dufouleur, C. Colombo, T. Garma et al., "P-Doping mechanisms in catalyst-free gallium arsenide nanowires," *Nano Letters*, vol. 10, no. 5, pp. 1734–1740, 2010.

[11] M. Hilse, M. Ramsteiner, S. Breuer, L. Geelhaar, and H. Riechert, "Incorporation of the dopants Si and Be into GaAs nanowires," *Applied Physics Letters*, vol. 96, no. 19, Article ID 193104, 2010.

[12] A. Casadei, P. Krogstrup, M. Heiss et al., "Doping incorporation paths in catalyst-free Be-doped GaAs nanowires," *Applied Physics Letters*, vol. 102, no. 1, Article ID 013117, 2013.

[13] l. Casadei, J. Schwender, E. Russo-Averchi et al., "Electrical transport in C-doped GaAs nanowires: surface effects," *Physica Status Solidi (RRL)—Rapid Research Letters*, vol. 7, no. 10, pp. 890–893, 2013.

[14] J. Dufouleur, C. Colombo, T. Garma et al., "P-doping mechanisms in catalyst-free gallium arsenide nanowires," *Nano Letters*, vol. 10, no. 5, pp. 1734–1740, 2010.

[15] H. J. Park, J. Kim, M. S. Kim et al., "Electrical characteristics of Mg-doped GaAs epitaxial layers grown by molecular beam

epitaxy," *Journal of Crystal Growth*, vol. 310, no. 10, pp. 2427–2431, 2008.

[16] C. E. C. Wood, D. Desimone, K. Singer, and G. W. Wicks, "Magnesium- and calcium-doping behavior in molecular-beam epitaxial III–V compounds," *Journal of Applied Physics*, vol. 53, no. 6, pp. 4230–4235, 1982.

[17] M. Mannoh, Y. Nomura, K. Shinozaki, M. Mihara, and M. Ishii, "Ionized Mg doping in molecular-beam epitaxy of GaAs," *Journal of Applied Physics*, vol. 59, no. 4, pp. 1092–1095, 1986.

[18] B. P. Falcão, J. P. Leitão, J. C. González et al., "Photoluminescence study of GaAs thin films and nanowires grown on Si(111)," *Journal of Materials Science*, vol. 48, no. 4, pp. 1794–1798, 2013.

[19] B. P. Falcão, J. P. Leitao, M. R. Correia et al., "Structural and optical characterization of Mg-doped GaAs nanowires grown on GaAs and Si substrates," *Journal of Applied Physics*, vol. 114, no. 18, Article ID 183508, 2013.

[20] B. P. Falcão, J. P. Leitão, M. R. Correia et al., "New insights into the temperature-dependent photoluminescence of Mg-doped GaAs nanowires and epilayers," *Journal of Materials Chemistry C*, vol. 2, no. 34, pp. 7104–7110, 2014.

[21] S. A. Dayeh, D. P. R. Aplin, X. Zhou, P. K. L. Yu, E. T. Yu, and D. Wang, "High electron mobility InAs nanowire field-effect transistors," *Small*, vol. 3, no. 2, pp. 326–332, 2007.

[22] Y. Huang, X. Duan, Y. Cui, and C. M. Lieber, "Gallium nitride nanowire nanodevices," *Nano Letters*, vol. 2, no. 2, pp. 101–104, 2002.

[23] D. R. Khanal and J. Wu, "Gate coupling and charge distribution in nanowire field effect transistors," *Nano Letters*, vol. 7, no. 9, pp. 2778–2783, 2007.

[24] O. Wunnick, "Gate capacitance of back-gated nanowire field-effect transistors," *Applied Physics Letters*, vol. 89, no. 8, Article ID 083102, 2006.

[25] J. C. González, G. M. Ribeiro, E. R. Viana et al., "Hopping conduction and persistent photoconductivity in Cu2ZnSnS4 thin films," *Journal of Physics D: Applied Physics*, vol. 46, no. 15, Article ID 155107, 2013.

[26] D. E. Hill, "Activation energy of holes in Zn-Doped GaAs," *Journal of Applied Physics*, vol. 41, no. 4, p. 1815, 1970.

[27] M. Wenzel, G. Irmer, J. Monecke, and W. Siegel, "Hole mobilities and the effective Hall factor in p-type GaAs," *Journal of Applied Physics*, vol. 81, no. 12, pp. 7810–7816, 1997.

[28] S. A. Stockman, G. E. Höfler, J. N. Baillargeon, K. C. Hsieh, K. Y. Cheng, and G. E. Stillman, "Characterization of heavily carbon-doped GaAs grown by metalorganic chemical vapor deposition and metalorganic molecular beam epitaxy," *Journal of Applied Physics*, vol. 72, no. 3, pp. 981–987, 1992.

[29] D. C. Look, *Electrical Characterization of GaAs Materials and Devices*, John Wiley & Sons, Great Britain, UK, 1989.

[30] E. R. Viana, J. C. González, G. M. Ribeiro, and A. G. D. Oliveira, "3D hopping conduction in SnO_2 nanobelts," *Physica Status Solidi—Rapid Research Letters*, vol. 6, no. 6, pp. 262–264, 2012.

[31] N. F. S. Mott and E. A. Davis, *Electronic Process in Non-Crystalline Materials*, Clarendon Press, Oxford, UK, 1979.

[32] B. I. Shklovskii and A. L. Efros, *Electronic Properties of Doped Semiconductors*, Springer, Berlin, Germany, 1984.